# Addition of biochar and trace elements in the form of industrial FeCl3 to stabilize anaerobic digestion of food waste: dosage optimization and long-term study

Gabriel Capson-Tojo, Chloé Girard, Maxime Rouez, Marion Crest,
Jean-Philippe Steyer, Nicolas Bernet, Jean-Philippe Delgenes, Renaud Escudié

# Biochar and industrial FeCl3 as additives to favor the consumption of volatile fatty acids during anaerobic digestion of food waste

| | |
|---|---|
| Journal: | *Journal of Chemical Technology & Biotechnology* |
| Manuscript ID | JCTB-18-0700 |
| Wiley - Manuscript type: | Research Article |
| Date Submitted by the Author: | 10-Jun-2018 |
| Complete List of Authors: | Capson-Tojo, Gabriel; LBE, INRA, Univ. Montpellier; Suez, CIRSEE Girard, Chloe; Suez, CIRSEE Rouez, Maxime; Suez, CIRSEE Crest, Marion; Suez, CIRSEE Steyer, Jean-Philippe; LBE, INRA, Univ. Montpellier Bernet, Nicolas; LBE, INRA, Univ. Montpellier Delgenès, Jean-Philippe; LBE, INRA, Univ. Montpellier Escudié, Renaud; LBE, INRA, Univ. Montpellier |
| Key Words: | Biogas, Anaerobic Digestion, Char, Design of Experiment (DOE) |
| | |

SCHOLARONE™
Manuscripts

1    **Biochar and industrial FeCl₃ as additives to favor the consumption of volatile fatty acids**

2    **during anaerobic digestion of food waste**

3

4    **Short title: Biochar and industrial FeCl₃ to stabilize the anaerobic digestion of food**

5    **waste**

6

7    Gabriel Capson-Tojo [a,b], Chloé Girard [b], Maxime Rouez [b], Marion Crest [b], Jean-Philippe

8    Steyer [a], Nicolas Bernet [a], Jean-Philippe Delgenès [a], Renaud Escudié [a,]*

9

10   [a] LBE, INRA, Univ. Montpellier, 102 avenue des Etangs, 11100 Narbonne, France

11   [b] Suez, CIRSEE, 38 rue du Président Wilson, 78230 Le Pecq, France

12   * Corresponding author: tel. +33 (0) 468.425.173, e-mail: *renaud.escudie@inra.fr*

13

14   **Abstract**

15   **BACKGROUND**

16   Although anaerobic digestion is a promising alternative for the valorization of complex

17   substrates such as food waste, this process is yet to be optimized and options for its

18   stabilization must be developed. The goal of this study was to assess for the first time if the

19   addition of biochar, together with trace elements in the form of an industrial FeCl₃ solution,

20   could serve as method for stabilizing anaerobic digestion of food waste.

21   **RESULTS**

22   Results from batch reactors demonstrated that the supplementation of both biochar and

23   industrial FeCl₃ favored the digestion kinetics. Their addition improved the maximum

24   methane production rates (from 886 up to 1498 ml·g $VS^{-1}·d^{-1}$) and the average daily methane

25   production rates (from 280 up to 376 ml·$d^{-1}$), related to acetate and propionate consumption,

26 respectively. Continuous reactors confirmed the batch results, with higher methane production

27 rates (up to 1.75 $l \cdot l^{-1} \cdot d^{-1}$) and lower concentrations of both acetate and propionate when

28 biochar and FeCl3 were added.

29 **CONCLUSION**

30 Addition of biochar and industrial FeCl3 favored the digestion kinetics, improving volatile

31 fatty acid consumption and the methane production rates. Although more research is needed,

32 these materials appear as an economically-feasible alternative for stabilizing the valorization

33 of food waste at industrial scale.

34

35 **Introduction**

36 The increasing production of food waste (FW) and novel international regulations call for the

37 development of novel sustainable technologies for its treatment and valorization (1). Among

38 the existing options, anaerobic digestion (AD) is an environmental-friendly process that

39 provides an efficient waste treatment, producing at the same time biogas and digestate.

40 Nevertheless, FW AD is a complex biological process that often leads to inefficient results or

41 reactor acidification. The first complication occurring during FW AD is related to the fast

42 biodegradability of this substrate, which is mainly composed of easily degradable

43 carbohydrates. Therefore, the reactors can be easily overloaded, especially in batch systems

44 (2), causing an unbalance between the acidogenesis/acetogenesis and the methanogenesis

45 steps, which results in an initial accumulation of volatile fatty acids (VFAs) and a consequent

46 pH drop (1,3–6). The second issue to be dealt with is related to the high protein content of this

47 substrate and its low water content (~20 % total solids; TS). During AD, organic nitrogen

48 (usually in the form of proteins) is reduced into ammonia nitrogen (total ammonia nitrogen;

49 TAN), which, in its free form (free ammonia nitrogen; FAN) is toxic to microorganisms,

50 especially to methanogenic archaea, eventually resulting also in an accumulation of VFAs.

51 Thus, different FW AD studies have reported inefficient performances due to high

52 concentrations of FAN (7–9).

53 The main alternative that has been applied to favor the consumption of VFAs in FW AD is the

54 supplementation of trace elements (TEs) (10–14). TEs have been found to favor VFA

55 consumption in both mesophilic and thermophilic AD of FW, mainly due to a favored

56 synthesis of critical enzymes in the process of syntrophic hydrogenotrophic methanogenesis

57 (HM), which is known to be the predominant methane-producing pathway during FW AD

58 (2,11,15–17). TEs addition has been successfully applied to avoid accumulation of VFAs at

59 high organic loading rates (OLRs) (10,18,19) and to recover acidified reactors (20,21).

60 Another strategy to favor VFA consumption during AD that has gained attention in the last

61 few years is the addition of conductive materials (22,23). This approach is based on the

62 capability of these materials for improving microbial interactions, by allowing the formation

63 of biofilm onto theirs surfaces and by facilitating the occurrence of direct interspecies electron

64 transfer (DIET), a mechanism in which the transfer of electrons between species occurs

65 through shared physical connections. DIET is a faster and more efficient route for electron

66 transfer than mediated interspecies electron transfer (23) and, as molecular hydrogen is no

67 longer formed, VFA oxidation is thermodynamically independent of its concentration (22,24).

68 Moreover, recent studies have suggested that acetic acid (HAc), butyric acid (HBu) and

69 propionic acid (HPr) can be metabolized through DIET (22,25–27). Materials such as

70 granular activated carbon (GAC), carbon cloth or magnetite have been found to favor VFA

71 consumption and methane production during AD (26,28,29). Among them, GAC appears as a

72 particularly performant alternative that has been found to promote the consumption of HAc,

73 HBu and HPr during AD of dog-food waste and FW (22,28,30).

74 However, both TEs and GAC are expensive and their application at an industrial scale is far

75 from being feasible. Thus, cheaper alternatives must be found. A simple substitute for the TEs

76    solution may be industrial $FeCl_3$, which consists on an acid solution, highly concentrated in

77    different metals (mainly Fe) that is commonly applied in wastewater treatment plants and

78    anaerobic digesters for pH control worldwide. Concerning GAC, an affordable substitute may

79    be biochar, which is also a carbon-conductive material with the capacity of accepting and

80    donating electrons (31). In addition, biochar may also improve the AD process by providing

81    buffering capacity and by sorption of inhibitors (32). It also favors nutrient retention in the

82    digestates, facilitating nutrient uptake if the digestate is spread on land for plant cultivation

83    (32,33). Moreover, as biochar can be produced from digestate (34) or directly from FW (35),

84    its addition for AD improvement clearly fits within the approach of environmental

85    biorefinery.

86    Biochar has been previously used as amendment for AD: (i) for biogas purification (removal

87    of $H_2S$ or $CO_2$) (36–38), (ii) as reactor packing for biofilm support (39), (iii) as AD substrate

88    (40), (iv) for nutrient supplementation (41), (v) as matrix for sorption of inhibitors (42,43) or

89    (vi) as means to increase the buffer capacity of the system (33). However, only three studies

90    have been carried out dealing with low-dosage of biochar for improving the AD kinetics. Luo

91    et al. (44) studied the addition of biochar for improving the kinetics of methane production

92    and VFA degradation (HAc and HBu) with glucose as substrate, concluding that a positive

93    effect existed. Zhao et al. (27) investigated the effect of biochar and ethanol supplementation

94    in reactors degrading HPr and HBu, observing that the degradation of both VFAs was

95    improved by adding biochar and concluding that bacteria known to participate in DIET (*i.e.*

96    *Geobacter* species) were attached onto the biochar surface. Finally, Sunyoto et al. (45)

97    assessed the influence of biochar addition in a two-phase AD reactor treating aqueous

98    carbohydrates FW, concluding that biochar supplementation increased the hydrogen and

99    methane production rates. They attributed this improvement to a promotion of the biofilm

100   formation.

101  To the knowledge of the authors, no study has been carried out so far to assess if addition of

102  biochar can favor VFA consumption during AD of complex substrates such as FW. Moreover,

103  the stabilizing effect of jointly adding industrial FeCl$_3$ (to provide TEs) and biochar on the

104  performance of FW AD has been investigated for the first time. Therefore, the goal of this

105  study was to: (i) optimize the concentrations of both biochar and industrial FeCl$_3$ using a

106  batch experimental design to improve the kinetics of FW AD and (ii) evaluate the effect of

107  industrial FeCl$_3$ and biochar supplementation on the AD performance of semi-continuous

108  pilot reactors treating commercial FW.

109

110  **Experimental**

111  _Inoculum, substrate and AD additives_

112  The reactors were inoculated with digestate from an industrial plant treating different organic

113  streams at high TAN/FAN concentrations (5.04 g TAN·l$^{-1}$; 615 mg FAN·l$^{-1}$). Thus, it was

114  assumed that the microorganisms would be adapted to high the high TAN/FAN levels

115  associated with FW AD (9). The TS content of the inoculum was $5.81 \pm 0.02$ %, with a

116  proportion of volatile solids (VS) of $59.13 \pm 0.08$ %. The activity of the inoculum was

117  verified prior its utilization using ethanol as substrate. The commercial FW was collected

118  from five mayor producers from the region of the Grand Narbonne, in the south of France. A

119  proportional mixture (wet weight) was used as substrate. The main characteristics of the FWs,

120  as well as those of the mixture used as substrate and the inoculum are presented in Table 1.

121  The characteristics of the FW mixture were in agreement with typical values presented in the

122  literature (1), which indicated that it could be considered as a representative sample of a

123  general FW. It had a TS contents of 21 % (90.3 % VS), it was mainly composed of

124  carbohydrates (618 g·kg TS$^{-1}$) and it had relatively low C/N ratios (16.1). No sulfur was

125  detected. A more extensive characterization and a deeper discussion of the results can be

126     found in Capson-Tojo et al. (9).

127     The industrial $FeCl_3$ was provided by an industrial AD plant, where it is still used for pH

128     controlling purposes. The characteristics and composition of this industrial solution, rich in

129     TEs, are shown in Table 2.

130     The biochar was natural slow-pyrolyzed wood charcoal, commonly found in the market for

131     several applications. Before utilization, the biochar was grinded and sieved at 600 μm.

132     *Batch experimental design for dosage optimization*

133     A multilevel factorial design was used to optimize the dosage of biochar and industrial $FeCl_3$

134     and to evaluate their individual effect on the methane production and the VFA production-

135     consumption kinetics. Digestate from continuous reactors digesting FW was used as inoculum

136     (after consumption of the remaining VFAs). This sludge had a TS content of 5.17 %, with

137     60.2 % corresponding to VS and had a TAN content of 7.27 $g·l^{-1}$. Sixty g of FW were added

138     as substrate in all the reactors. A substrate to inoculum (S/X) ratio of 1 g VS·g $VS^{-1}$ was

139     applied, leading to initial FW concentrations of approximately 27 g FW·$l^{-1}$. The reactors

140     were incubated at 37 °C. The working volumes ranged from 487 ml to 529 ml. Two different

141     concentrations of the $FeCl_3$ solution (0.1 and 0.2 g Fe·$l^{-1}$) and three of biochar (10, 55 and 100

142     $g·l^{-1}$) were tested. As a result, an experimental design with 12 conditions was defined (6

143     conditions in duplicate; Table 3). Two consecutive batch feeding were carried out. The first

144     feeding served for inoculum adaptation (results not presented), and the results of the second

145     one were used for modelling purposes. It must be mentioned that, based on previous results, it

146     was decided not to include into the experimental design reactors containing only biochar and

147     $FeCl_3$. As it was demonstrated in Capson-Tojo et al. (30), although the separate addition of

148     GAC and TEs also enhanced the VFAs degradation kinetics during FW AD, the best

149     performances were achieved when both of these reagents were added simultaneously. With

150     these results as starting point, the current experimental designed was defined. The same study

151 was also used to define the levels of industrial $FeCl_3$ and biochar to be tested (30).

152 This experimental design was chosen because it allows analyzing the effects of the selected

153 factors (biochar and $FeCl_3$ concentrations) on a chosen output through the entire experimental

154 region covered. This implied that it was possible to distinguish between the effect of biochar

155 and $FeCl_3$ without the need of single additive treatments. It allows so by predicting the

156 responses using a quadratic model (Eq. 1):

157

158
$$y = a_0 + \sum_{i-1}^{k} a_i \cdot x_i + \sum_{i-1}^{k} a_{ii} \cdot x_i^2 + \sum_{i<j}^{k} a_{ij} \cdot x_i \cdot x_j \qquad \text{Equation 1}$$

159

160 Where y is the response to be predicted, $x_i$ are the studied factors and $a_i$, $a_{ii}$ and $a_{ij}$ are the

161 parameters corresponding to each factor. These parameters represent the linear effects, the

162 quadratic effects and the interactional effects, respectively. The first coefficient $a_0$ is required

163 for fitting the mathematical model. The p-values from F-tests (95 % confidence) and the

164 coefficient of determination $R^2$ were used to evaluate the fitness of the model. The experiment

165 was designed and evaluated using the software STATGRAPHICS Centurion XVI Version

166 16.1.03 (©StatPoint Technologies Inc.).

167 The reactors were incubated in an Automated Methane Potential Testing System (AMPTSII)

168 (Bioprocess Control, Sweden). Twelve reactors from the AMPTSII system, with a total

169 volume of 600 ml, were used. According to the manufacturer instructions, they were

170 connected to $CO_2$ traps (NaOH solutions) and to gas flow meters to determine continuously

171 the methane flow rates. These reactors also allowed the follow-up of the dynamics of VFA

172 production-consumption. A hole present in each vessel was used as sampling port, facilitating

173 an easy sampling of the digestate. The reactors were agitated during one minute every 10

174 minutes at 40 rpm.

175 The criterion followed to decide when the batch had finished was the total consumption of the

176    HPr in the reactors (26 days). Blank reactors (without substrate addition) were carried out to

177    account for the endogenous respiration of the inoculum.

178    *Continuous pilot scale reactors*

179    In parallel to the batch reactors, two different pilot scale reactors were run: a control system

180    simply digesting FW and a doped reactor supplemented with biochar and the $FeCl_3$ solution.

181    Both reactors were incubated at 37 °C and had a working volume of 12 l. The reactors were

182    fed once per day, initially with an OLR of 1.4 g $VS \cdot l^{-1} \cdot d^{-1}$, corresponding to a hydraulic

183    retention time (HRT) of 110 days. This value was increased to 2.8 g $VS \cdot l^{-1} \cdot d^{-1}$ (HRT of 55

184    days) after 77 days of operation. An equivalent amount of digestate was withdrawn to keep

185    the volume of the reactors constant. The $FeCl_3$ solution was diluted with water (x20 vol:vol)

186    and dosed into the supplemented reactor to keep a constant concentration of 100 mg $Fe \cdot l^{-1}$

187    (value calculated from optimal results reported in the literature (10–12)). This corresponded to

188    concentrations of 0.38 mg $Mn \cdot l^{-1}$, 0.19 mg $Zn \cdot l^{-1}$, 0.03 mg $Ni \cdot l^{-1}$, 0.01 mg $Co \cdot l^{-1}$ and 0.01 mg

189    $Mg \cdot l^{-1}$ in the reactor. The initial concentration of biochar in the supplemented reactor was 10

190    $g \cdot l^{-1}$. As it will be further explained, this concentration was increased up to 50 $g \cdot l^{-1}$ to favor the

191    consumption of the accumulated VFAs, according to the results obtained from the batch

192    experimental design.

193    The pilot reactors consisted of jacketed cylindrical vessels made of stainless steel that had

194    inner stirring blades to provide continuous agitation. A more detailed description of the

195    reactors can be found elsewhere (9). The experiments lasted for 196 days.

196    *Analytical methods*

197    *Physico-chemical characterization of the FW*

198    The TS and VS contents were measured as described in the standard methods of the American

199    Public Health Association (46). The concentrations of carbohydrates and lipids were

200    determined using the Dubois method (47) and by a gravimetric method based on accelerated

201    solvent extraction (46), respectively. The protein content was calculated using the total

202    Kjeldahl nitrogen (TKN) contents (6.25 g protein·g $N^{-1}$ (48)). The TKN and $NH_4^+$

203    concentrations were determined using an AutoKjehdahl Unit K-370, BUCHI. The contents of

204    organic (TOC) and inorganic carbon (IC) were measured with a Shimadzu (Kyoto, Japan)

205    TOC-$V_{CSN}$ Total Organic Carbon Analyzer coupled to a Shimadzu ASI-V tube rack. The C/N

206    ratio was calculated as TOC/TKN. A WTW (London, United Kingdom) pHmeter series

207    inoLab pH720 was used for pH measurement. Finally, the biochemical methane potentials

208    (BMPs) of the substrates were measured according to Motte et al. (49).

209    *Gas quantification and analysis*

210    The amount of methane produced was automatically measured in the AMPTSII system and

211    the volume of biogas produced in the pilot reactors was continuously measured using Ritter

212    MilliGascounters MGC-1 V3.0. The composition of the biogas was determined by gas

213    chromatography as described in Cazier et al. (50).

214    *Analysis of metabolites and final products of the digestion*

215    A sample of digestate from the pilot reactors was taken once per week for measurement of the

216    concentrations of VFAs and ionic species in the reactors. Concerning the batch study, a

217    plastic tube submerged in the reaction media served for digestate sampling when required.

218    Before sampling, a clip was used for blocking the gas output and the equivalent volume of

219    digestate to be removed was injected as nitrogen gas, avoiding an overestimation of the

220    produced gas. The concentrations of VFAs and ionic species in the digestates were measured

221    as described in Motte et al. (51), by gas and ion chromatography, respectively.

222    <u>*Data analysis*</u>

223    The concentration of FAN was calculated according to Chen et al. (52) as a function of

224    temperature, pH, and TAN concentration.

225    The methane yields were calculated by dividing the total volume of methane produced by the

226  initial mass of VS of substrates. They were corrected to take into account the digestate

227  removed when sampling. The concentrations of FAN in the reactors were determined

228  according to Rajagopal et al. (8), as a function of temperature, pH, ionic strength and TAN

229  concentration. The concentrations of the main ions present in the reactors (Cl$^-$, Na$^+$, NH$_4^+$, K$^+$,

230  Mg$^{2+}$, H$^+$, VFAs and Ca$^{2+}$) were taken into account in this calculation.

231

**Results and discussion**

233  *Optimization of biochar and FeCl$_3$ dosing in batch reactors*

234  As aforementioned, the first objective of this study was to evaluate the effect of different

235  concentrations of both biochar and industrial FeCl$_3$, aiming at optimizing their dosage. The

236  results of the experimental design (using the second consecutive batch) are shown in Table 4.

237  All the reactors produced methane efficiently, with yields ranging from 456 to 505 ml CH$_4$·g

238  VS$^{-1}$ and final pH values between 8.15 and 8.42. These high pH values were caused by the

239  high TAN concentrations, up to 9.75 g·l$^{-1}$. As it can be observed, the main differences were

240  related to the AD kinetics. The maximum methane production rates (consequence of the

241  initial consumption of HAc) varied widely, from 907 to 1498 ml·g VS$^{-1}$·d$^{-1}$. The total time for

242  consumption of HPr (most recalcitrant VFA to be degraded) ranged from 18.9 to 24.4 days.

243  The average daily methane production was calculated by dividing the total volume of methane

244  produced by the batch duration (*i.e.* time to completely degrade HPr), according to Capson-

245  Tojo et al. (30). It varied from 302 to 376 ml CH$_4$·d$^{-1}$. The values of the methane yields, the

246  maximum methane rates and the average daily methane production rates were used as inputs

247  for the quadratic model (Equation 1), obtaining the results presented in Table 5. The raw

248  kinetic curves of the methane yields and production rates, the pH values and the

249  concentrations of the different VFAs are presented in Figure S1 and Figure S2 (supplementary

250  material).

251    Starting with the methane yields, the modeled results indicated that both linear coefficients

252    from the biochar and the $FeCl_3$ (*i.e.* $a_{biochar}$ and $a_{FeCl3}$) had a significant effect on this variable

253    (p-values linear coefficients $< 0.05$). However, the quadratic parameter $a_{biochar-biochar}$ was

254    statistically different than zero with a 99 % of certainty (p-value $< 0.01$) and the high value of

255    this parameter indicated that the experimental design was not properly centered for predicting

256    the methane yield. The relatively low $R^2$ value (86.7 %) also suggests the lack of fit of the

257    model. In addition, the Durbin-Wilson test (with a p-value $< 0.05$) could not exclude that

258    correlations existed due to the order in which the data were used as input. All these results

259    suggest that the model was not able to predict any direct effect of the biochar or the $FeCl_3$ on

260    the final methane yields obtained, indicating that no significant differences existed between

261    the obtained results. Considering that the biodegradable matter content of these two additives

262    should be negligible, this is a logical outcome.

263    Nevertheless, the model was able to reproduce precisely the maximum methane production

264    rates ($R^2$ of 94.2 % and p-value Durbin-Wilson 0.20) and the average daily methane

265    production rates ($R^2$ of 100 %), indicating that highly significant differences existed between

266    the reactors. The model responses for these two variables are presented in Figure 1.

267    The maximum methane production rate was mainly affected by the biochar concentration,

268    with a negligible influence of the industrial $FeCl_3$ concentration. This can be verified by the p-

269    values of the parameters in Table 5, where it can be observed that the only parameter with a p-

270    value $< 0.5$ was $a_{biochar}$. This indicates that addition of biochar clearly improved the

271    degradation of the HAc that accumulated at the beginning of the AD process, when the

272    maximum methane production rates were registered (Figure S1 and Figure S2). This is in

273    agreement with previous results, where GAC addition enhanced the HAc consumption during

274    batch FW AD (30). Regarding the average daily methane production rates (estimated by

275    dividing the total volume of methane produced by the time to completely degrade the HPr),

276    the value of this variable also increased greatly at higher biochar concentrations. However, in

277    this case the effect of the $FeCl_3$ was significant, with both $a_{biochar}$ and $a_{FeCl3}$ showing p-values

278    lower than 0.5. This variable was mainly affected by the batch duration, which was

279    determined by the time required for HPr consumption. Thus, it can be concluded that both

280    biochar and industrial $FeCl_3$ addition favored the degradation of the HPr accumulated during

281    the first days of the batch process. This can be related to favored syntrophic interactions and

282    to the occurrence of DIET in the case of biochar and to the synthesis of enzymes for the

283    industrial $FeCl_3$ (*i.e.*, TEs contained in this solution). Again, this is in agreement with

284    previous results presented in the literature. Adding GAC and TEs into batch reactors, a

285    reduction of the time required to completely degraded the accumulated HPr of around 40 %

286    was observed during batch FW AD (30).

287    Although optimal values could be extrapolated (162 $g \cdot l^{-1}$ of biochar at 0.1 g $Fe \cdot l^{-1}$ for

288    maximizing the methane production rate and 111 $g \cdot l^{-1}$ of biochar at 0.2 g $Fe \cdot l^{-1}$ for

289    maximizing the average methane production rates), it is clear that the experimental design

290    was no properly centered and therefore further experiments must be performed to precisely

291    optimize the dosing of these reagents.

292    *Performance of the continuous pilot reactors*

293    Two continuous pilot reactors were run in parallel to the batch reactors during 196 days: a

294    control reactor fed only with FW and a reactor supplemented with biochar and industrial

295    $FeCl_3$. The main operational parameters and the obtained results are presented in Figure 2.

296    After starting the reactors at an OLR of 1.4 g $VS \cdot l^{-1} \cdot d^{-1}$, it was required to wait around 30-40

297    days to achieve a stable methane production of 10 $l \cdot d^{-1}$ in both systems. Interestingly,

298    differences between both reactors could already be appreciated in this start-up period. After

299    15 days, the reactor supplemented with biochar and industrial $FeCl_3$ showed higher methane

300    production rates than the control (Figure 2B), which were associated with higher initial

301    methane yields, lower concentrations of HAc and HPr (*i.e.* peaks of HAc of 13 and 16 $g \cdot l^{-1}$,

302    respectively) and higher pH values. This suggests that the added AD enhancers favored the

303    consumption of the VFAs accumulated during the start-up period, even at a biochar

304    concentration of 10 $g \cdot l^{-1}$. This is in agreement with the batch results, confirming the positive

305    effect of adding these reagents on the initial HAc consumption (leading to a lower extent of

306    HPr accumulation) and on the HPr degradation.

307    Moving forwards, after 60 days both reactors achieved efficient methane productions at the

308    first OLR applied, with yields around 400 ml $CH_4 \cdot g$ $VS^{-1}$ (95 % of the BMP), with relatively

309    low concentrations of VFAs in the reactors (2 $g \cdot l^{-1}$ of HAc and 0.3 $g \cdot l^{-1}$ for HPr) and with high

310    pH values (around 8.1). It must be mentioned that high TAN concentrations were already

311    present in the reactors at this point, with values around 8 $g \cdot l^{-1}$ in both reactors at day 68. It

312    must also be commented that the average TAN concentrations in the reactors were $8513 \pm 362$

313    $mg \cdot l^{-1}$ in control reactor and $8432 \pm 777$ $mg \cdot l^{-1}$ in the biochar-supplemented reactor

314    (corresponding to 398 and 550 mg $FAN \cdot l^{-1}$, respectively). This indicates that no significant

315    differences existed and that the observed improvement of the AD performance was no caused

316    by a reduction in the TAN/FAN concentrations related to its adsorption on the biochar

317    particles.

318    However, due to the low OLR applied, relatively low methane production rates (around 10 l

319    $CH_4 \cdot d^{-1}$) were obtained. Therefore, the OLR was doubled in day 77 to reach 2.8 g $VS \cdot l^{-1} \cdot d^{-1}$.

320    This caused a sudden drop in the methane yields to 160 ml $CH_4 \cdot g$ $VS^{-1}$, which was associated

321    with an increase in the HAc and HPr concentrations in the reactors. In agreement with the

322    previous results, the levels of both VFAs were always lower in the supplemented reactor.

323    In an attempt to reduce the intensity of VFA accumulation in the reactor containing biochar

324    and $FeCl_3$, the biochar concentrations were increased to 20 $g \cdot l^{-1}$ on day 105 and to 50 $g \cdot l^{-1}$ on

325    day 146 (based on the results from the batch optimization experiment described above). While

326  the first increase did not have significant effects, the second one (to 50 $g \cdot l^{-1}$) caused a drop in

327  the HAc concentration from 13 to 7 $g \cdot l^{-1}$, raising the methane yields up to 350 ml $CH_4 \cdot g\ VS^{-1}$.

328  A consequent decrease in the HPr concentration was observed (from 3.1 to 1.8 $g \cdot l^{-1}$). Sadly,

329  on day 167 a problem occurred with the heating of the biochar-supplemented reactor. This

330  caused a temperature drop, which led to a sudden decrease of the methane yields obtained

331  and, again, an accumulation of HAc at the end of the operational period (days 167 to 196).

332  Besides the aforementioned complication, Figure 2 clearly shows that addition of biochar and

333  industrial $FeCl_3$ decreased the HPr concentrations in reactors, with considerable differences

334  between the supplemented reactor and the control. This discrepancy was particularly

335  important after increasing the biochar concentrations, with HPr levels of 7.2 $g \cdot l^{-1}$ in the

336  control reactor and of 1.8 $g \cdot l^{-1}$ in the reactor containing biochar and industrial $FeCl_3$ at the end

337  of the operational period.

338  Although the obtained results further suggest that addition of biochar and industrial $FeCl_3$ can

339  improve the AD kinetics and favor VFA consumption during FW AD, it is also clear that

340  further continuous experiments must be carried out, allowing longer operational periods.

341  These experiments should aim to reach an operational steady-state, with results that can be

342  extrapolated to a potential industrial-scale facility.

343  *Biochar as feasible option for enhancing FW AD*

344  The results obtained both in batch and continuous reactors are in agreement with different

345  studies carried out to study the effect of biochar on AD. The kinetics of consumption of HAc

346  and HBu were reported to be faster when adding biochar using glucose as substrate (44). Also

347  the direct degradation of HPr and HBu has been improved by supplementing biochar and

348  ethanol (27). Sunyoto et al. (45) observed that biochar supplementation increased the methane

349  production rates and enhanced the consumption of HAc and HBu in the second stage of a 2-

350  phase AD reactor treating aqueous FW.

351  Using GAC as carbon-based AD enhancer, different studies have suggested that HAc, HBu

352  and HPr can be directly metabolized through DIET, improving the kinetics of consumption of

353  these VFAs (22,25–27). In addition, biochar has also been found to promote the growth of

354  bacteria known to participate in DIET (*i.e. Geobacter* species) onto its surface (27).

355  Therefore, it can be hypothesized that the improved VFA degradation kinetics could be

356  related to an enhancement of the syntrophic interactions between microorganisms via biofilm

357  formation and to the occurrence of DIET. The degradation of HAc through DIET has already

358  been proposed in the literature and, although being more limited thermodynamically (9),

359  DIET may have also played an important role in the oxidation of HPr. Besides, even if direct

360  DIET of HPr might not have occurred extensively, its degradation would be favored anyway

361  due to lower HAc and hydrogen/formate concentrations. Further studies analyzing the

362  microbial communities attached on the biochar, as well as the properties of the biochar used,

363  should be performed to verify this hypothesis. Concerning the industrial $FeCl_3$ addition, this

364  additive favored the HPr degradation due to the supplementation of TEs, critical for enzyme

365  synthesis (11).

366  These experiments proved that a regular biochar (natural slow-pyrolyzed wood charcoal)

367  could also improve greatly the AD performance using complex FW as substrate. It must also

368  be considered that, other than the concentration applied, many parameters and variables which

369  have not been considered in this study have a huge potential for optimization when

370  considering biochar as AD enhancer. It is clear that the textural characteristics of the biochar

371  (*e.g.* specific surface, pore volume, pore size or pore distribution) as well as its surface

372  chemistry (*e.g.* hydrophobicity) or its particle size play a major role on biofilm formation. In

373  addition, also its resistivity (conductivity) might have a huge impact on its capability for

374  favoring DIET. All these characteristics are dependent on different variables that clearly

375  deserve further study, such as the raw material used for biochar production (41), the

376    temperature and pressure applied during pyrolysis (*i.e.* slow or fast pyrolysis) or the

377    pretreatment applied to the biochar before its addition into the AD reactor (*i.e.* mechanical

378    grinding) (32).

379    Although deep techno-economic analyses must be carried out before considering its

380    application at industrial scale (particularly at the high concentrations of biochar applied,

381    which would require recirculation of the solid fraction of the digestate for biochar

382    reutilization), the obtained results suggest for the first time that biochar and industrial $FeCl_3$

383    can be a feasible alternative for stabilizing AD of FW, favoring the consumption of VFAs and

384    improving the methane productivities. When compared to substrate dilution (1:1 vol:vol),

385    which is the most commonly applied stabilization method in industrial facilities (increasing

386    greatly the HRTs and the volumes of digestate produced and requiring an input of clean

387    water), the proposed technology is clearly a more environmental-friendly option that can be

388    coupled with other waste treatment processes (*i.e.* green waste pyrolysis).

389

394

395    **References**

396    1.      Capson-Tojo G, Rouez M, Crest M, Steyer J-P, Delgenès J-P, Escudié R. Food waste

397    valorization via anaerobic processes: a review. *Rev Environ Sci Bio/Technology* **15** (3): 499–

398    547 (2016).

399    2.      Capson-Tojo G, Trably E, Rouez M, Crest M, Steyer J-P, Delgenès J-P, et al. Dry

400    anaerobic digestion of food waste and cardboard at different substrate loads, solid contents

401   and co-digestion proportions. *Bioresour Technol* **233**: 166–75 (2017).

402   3.      Capson-Tojo G, Rouez M, Crest M, Trably E, Steyer J, Bernet N, et al. Kinetic study

403   of dry anaerobic co-digestion of food waste and cardboard for methane production. *Waste*

404   *Manag* **69**: 470–479 (2017).

405   4.      Stabnikova O, Ang S, Liu X, Ivanov V, Tay J, Wang J. The use of hybrid anaerobic

406   solid–liquid (HASL) system for the treatment of lipid-containing food waste. *J Chem Technol*

407   *Biotechnol* **80** (4): 455–461 (2005).

408   5.      Kim HJ, Kim SH, Choi YG, Kim GD, Chung TH. Effect of enzymatic pretreatment

409   on acid fermentation of food waste. *J Chem Technol Biotechnol* **81** (6) :974–980 (2006).

410   6.      Wang XQ, Wang QH, Ma HZ, Yin W. Lactic acid fermentation of food waste using

411   integrated glucoamylase production. *J Chem Technol Biotechnol* **84** (1): 139–143 (2008).

412   7.      Banks CJ, Chesshire M, Stringfellow A. A pilot-scale trial comparing mesophilic and

413   thermophilic digestion for the stabilisation of source segregated kitchen waste. *Water Sci*

414   *Technol* **58** (7): 1475–1481 (2008).

415   8.      Rajagopal R, Massé DI, Singh G. A critical review on inhibition of anaerobic

416   digestion process by excess ammonia. *Bioresour Technol* **143** (0): 632–641 (2013).

417   9.      Capson-Tojo G, Ruiz D, Rouez M, Crest M, Steyer J-P, Bernet N, et al.

418   Accumulation of propionic acid during consecutive batch anaerobic digestion of commercial

419   food waste. *Bioresour Technol* **245**: 724–733 (2017).

420   10.     Zhang W, Zhang L, Li A. Enhanced anaerobic digestion of food waste by trace metal

421   elements supplementation and reduced metals dosage by green chelating agent [S, S]-EDDS

422   via improving metals bioavailability. *Water Res* **84**: 266–277 (2015).

423   11.     Banks CJ, Zhang Y, Jiang Y, Heaven S. Trace element requirements for stable food

424   waste digestion at elevated ammonia concentrations. *Bioresour Technol* **104** (0): 127–135

425   (2012).

426    12.    Zhang L, Jahng D. Long-term anaerobic digestion of food waste stabilized by trace

427    elements. *Waste Manag* **32** (8): 1509–1515 (2012).

428    13.    Voelklein MA, O'Shea R, Jacob A, Murphy JD. Role of trace elements in single and

429    two-stage digestion of food waste at high organic loading rates. *Energy* **121**: 185-192 (2017).

430    14.    Facchin V, Cavinato C, Fatone F, Pavan P, Cecchi F, Bolzonella D. Effect of trace

431    element supplementation on the mesophilic anaerobic digestion of food waste in batch trials:

432    The influence of inoculum origin. *Biochem Eng J* **70** (0): 71–77 (2013).

433    15.    Yirong C, Heaven S, Banks CJ. Effect of a Trace Element Addition Strategy on

434    Volatile Fatty Acid Accumulation in Thermophilic Anaerobic Digestion of Food Waste.

435    *Waste Biomass Valor* **6** (1):1–12 (2015).

436    16.    Westerholm M, Levén L, Schnürer A. Bioaugmentation of syntrophic acetate-

437    oxidizing culture in biogas reactors exposed to increasing levels of ammonia. *Appl Environ*

438    *Microbiol* **78** (21): 7619–7625 (2012).

439    17.    Capson-Tojo G, Trably E, Rouez M, Crest M, Bernet N, Steyer J-P, et al.

440    Methanosarcina plays a main role during methanogenesis of high-solids food waste and

441    cardboard. *Waste Manag* **76**: 423–430 (2018).

442    18.    Zhang W, Wu S, Guo J, Zhou J, Dong R. Performance and kinetic evaluation of semi-

443    continuously fed anaerobic digesters treating food waste: role of trace elements. *Bioresour*

444    *Technol* **178**: 297–305 (2015).

445    19.    Zhang L, Lee Y-W, Jahng D. Anaerobic co-digestion of food waste and piggery

446    wastewater: Focusing on the role of trace elements. *Bioresour Technol* **102** (8): 5048–5059

447    (2011).

448    20.    Qiang H, Lang D-L, Li Y-Y. High-solid mesophilic methane fermentation of food

449    waste with an emphasis on Iron, Cobalt, and Nickel requirements. *Bioresour Technol* **103** (1):

450    21–27 (2012).

451    21.    Qiang H, Niu Q, Chi Y, Li Y. Trace metals requirements for continuous thermophilic

452    methane fermentation of high-solid food waste. *Chem Eng J* **222**: 330–336 (2013).

453    22.    Dang Y, Holmes DE, Zhao Z, Woodard TL, Zhang Y, Sun D, et al. Enhancing

454    anaerobic digestion of complex organic waste with carbon-based conductive materials.

455    *Bioresour Technol.* **220**: 516–522 (2016).

456    23.    Lovley DR. Syntrophy Goes Electric: Direct Interspecies Electron Transfer. *Annu Rev*

457    *Microbiol* 29 (2017)

458    24.    Lee JY, Lee SH, Park HD. Enrichment of specific electro-active microorganisms and

459    enhancement of methane production by adding granular activated carbon in anaerobic

460    reactors. *Bioresour Technol* **205** :205–122 (2016).

461    25.    Zhao Z, Zhang Y, Yu Q, Dang Y, Li Y, Quan X. Communities stimulated with

462    ethanol to perform direct interspecies electron transfer for syntrophic metabolism of

463    propionate and butyrate. *Water Res* **102**: 475–484 (2016).

464    26.    Cruz Viggi C, Rossetti S, Fazi S, Paiano P, Majone M, Aulenta F. Magnetite particles

465    triggering a faster and more robust syntrophic pathway of methanogenic propionate

466    degradation. *Environ Sci Technol* **48** (13): 7536–7543 (2014).

467    27.    Zhao Z, Zhang Y, Holmes DE, Dang Y, Woodard TL, Nevin KP, et al. Potential

468    enhancement of direct interspecies electron transfer for syntrophic metabolism of propionate

469    and butyrate with biochar in up-flow anaerobic sludge blanket reactors. *Bioresour Technol*

470    **209**: 148–156 (2016).

471    28.    Dang Y, Sun D, Woodard TL, Wang L-Y, Nevin KP, Holmes DE. Stimulation of the

472    anaerobic digestion of the dry organic fraction of municipal solid waste (OFMSW) with

473    carbon-based conductive materials. *Bioresour Technol* **238**: 30–38 (2016).

474    29.    Zhang J, Zhang L, Loh K-C, Dai Y, Tong YW. Enhanced anaerobic digestion of food

475    waste by adding activated carbon: Fate of bacterial pathogens and antibiotic resistance genes.

476    *Biochem Eng J* **128**: 19–25 (2017).

477    30.      Capson-Tojo G, Moscoviz R, Ruiz D, Santa-Catalina G, Trably E, Rouez M, et al.

478    Addition of granular activated carbon and trace elements to favor volatile fatty acid

479    consumption during anaerobic digestion of food waste. *Bioresour Technol* **260**: 157–168

480    (2018).

481    31.      Prévoteau A, Ronsse F, Cid I, Boeckx P, Rabaey K. The electron donating capacity of

482    biochar is dramatically underestimated. *Sci Rep* **6**: 32870.

483    32.      Fagbohungbe MO, Herbert BMJ, Hurst L, Ibeto CN, Li H, Usmani SQ, et al. The

484    challenges of anaerobic digestion and the role of biochar in optimizing anaerobic digestion.

485    *Waste Manag*  **61**: 236–249 (2017).

486    33.      Wang D, Ai J, Shen F, Yang G, Zhang Y, Deng S, et al. Improving anaerobic

487    digestion of easy-acidification substrates by promoting buffering capacity using biochar

488    derived from vermicompost. *Bioresour Technol* **227**: 286–296 (2017).

489    34.      Monlau F, Sambusiti C, Antoniou N, Barakat A, Zabaniotou A. A new concept for

490    enhancing energy recovery from agricultural residues by coupling anaerobic digestion and

491    pyrolysis process. *Appl Energy* **148**: 32–38 (2015).

492    35.      Rago YP, Surroop D, Mohee R. Assessing the potential of biofuel (biochar)

493    production from food wastes through thermal treatment. *Bioresour Technol* **248**: 258-264

494    (2018).

495    36.      Linville JL, Shen Y, Ignacio-de Leon PA, Schoene RP, Urgun-Demirtas M. In-situ

496    biogas upgrading during anaerobic digestion of food waste amended with walnut shell biochar

497    at bench scale. *Waste Manag Res* **35**: 669-679 (2017).

498    37.      Shen Y, Linville JL, Ignacio-de Leon PAA, Schoene RP, Urgun-Demirtas M.

499    Towards a sustainable paradigm of waste-to-energy process: Enhanced anaerobic digestion of

500    sludge with woody biochar. *J Clean Prod* **135**: 1054–1064 (2016).

501 38. Shen Y, Linville JL, Urgun-Demirtas M, Schoene RP, Snyder SW. Producing

502 pipeline-quality biomethane via anaerobic digestion of sludge amended with corn stover

503 biochar with in-situ CO2 removal. *Appl Energy* **158**: 300–309 (2015).

504 39. Cooney MJ, Lewis K, Harris K, Zhang Q, Yan T. Start up performance of biochar

505 packed bed anaerobic digesters. *J Water Process Eng* **9**: e7–13 (2016).

506 40. Mumme J, Srocke F, Heeg K, Werner M. Use of biochars in anaerobic digestion.

507 *Bioresour Technol* **164**: 189–197 (2014).

508 41. Shen Y, Forrester S, Koval J, Urgun-Demirtas M. Yearlong semi-continuous

509 operation of thermophilic two-stage anaerobic digesters amended with biochar for enhanced

510 biomethane production. *J Clean Prod* **167**: 863-874 (2017).

511 42. Fagbohungbe MO, Herbert BMJ, Hurst L, Li H, Usmani SQ, Semple KT. Impact of

512 biochar on the anaerobic digestion of citrus peel waste. *Bioresour Technol* **216**: 142–149

513 (2016).

514 43. Torri C, Fabbri D. Biochar enables anaerobic digestion of aqueous phase from

515 intermediate pyrolysis of biomass. *Bioresour Technol* **172**: 335–341 (2014).

516 44. Luo C, Lü F, Shao L, He P. Application of eco-compatible biochar in anaerobic

517 digestion to relieve acid stress and promote the selective colonization of functional microbes.

518 *Water Res* **68**: 710–718 (2015)

519 45. Sunyoto NMS, Zhu M, Zhang Z, Zhang D. Effect of biochar addition on hydrogen

520 and methane production in two-phase anaerobic digestion of aqueous carbohydrates food

521 waste. *Bioresour Technol* **219**: 29–36 (2016).

522 46. APHA. Standard Methods for the Examination of Water and Wastewater. 21st ed.

523 Washington, DC: American Public Health Association; 2005.

524 47. Dubois M, Gilles KA, Hamilton JK, Rebers PA, Smith F. Colorimetric Method for

525 Determination of Sugars and Related Substances. *Anal Chem* **28** (3): 350–356 (1956).

526   48.     Jimenez J, Vedrenne F, Denis C, Mottet A, Déléris S, Steyer J-P, et al. A statistical

527   comparison of protein and carbohydrate characterisation methodology applied on sewage

528   sludge samples. *Water Res* **47** (5): 1751–1762 (2013).

529   49.     Motte J-C, Escudié R, Beaufils N, Steyer J-P, Bernet N, Delgenès J-P, et al.

530   Morphological structures of wheat straw strongly impacts its anaerobic digestion. *Ind Crops*

531   *Prod* **52**: 695–701 (2014).

532   50.     Cazier EA, Trably E, Steyer JP, Escudie R. Biomass hydrolysis inhibition at high

533   hydrogen partial pressure in solid-state anaerobic digestion. *Bioresour Technol* **190**: 106–113

534   (2015).

535   51.     Motte J-C, Trably E, Escudié R, Hamelin J, Steyer J-P, Bernet N, et al. Total solids

536   content: a key parameter of metabolic pathways in dry anaerobic digestion. *Biotechnol*

537   *Biofuels* **6** (1): 164 (2013).

538   52.     Chen JL, Ortiz R, Steele TWJ, Stuckey DC. Toxicants inhibiting anaerobic digestion:

539   a review. *Biotechnol Adv* **32** (8): 1523–34 (2014).
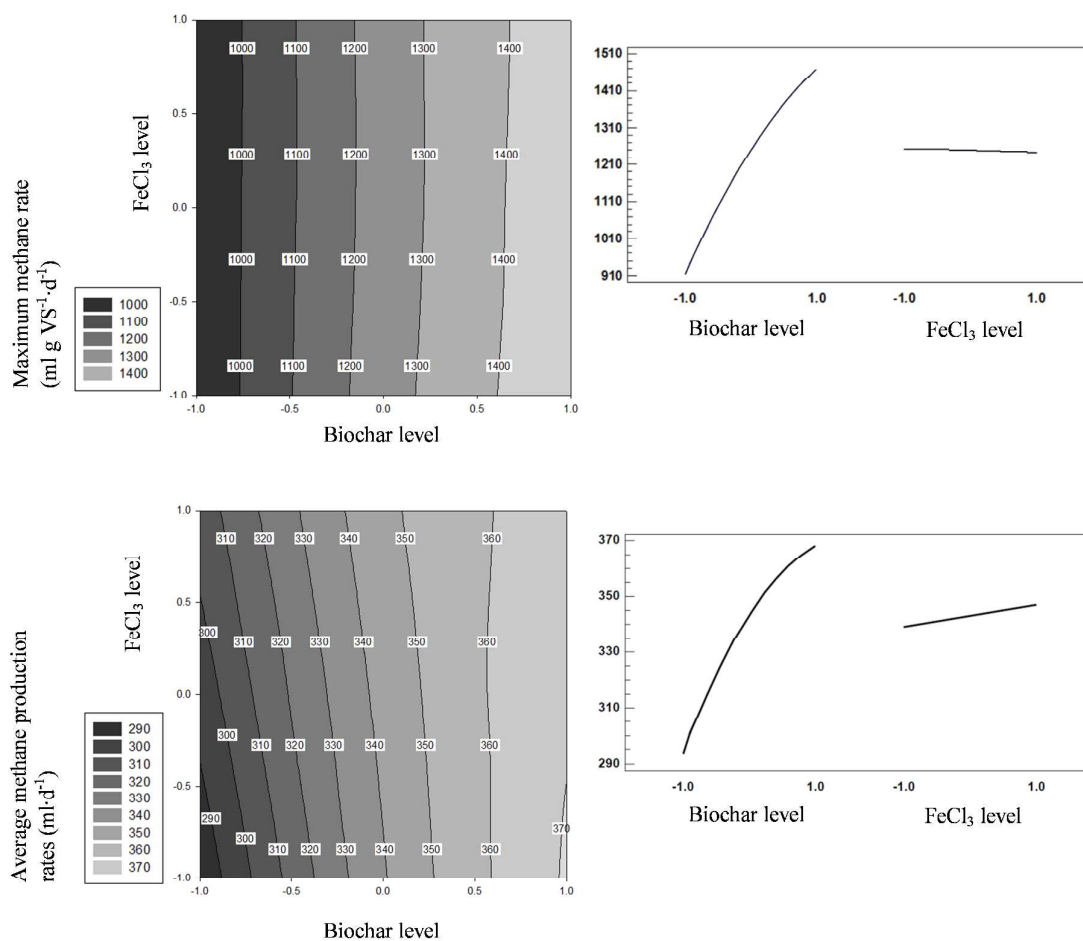
540

541

542

543

544

545

546

547

548

549

550

551 **Figure and Table captions**

552

553

554

555

556

557

558

559

560

561

562

563

564

565 **Figure 1.** Surface responses (left) and average individual effects (right) of (up) the maximum

566 methane rates and (down) the average daily methane production rates

567

568

569

570

571

572

573

574

575

576

577

578
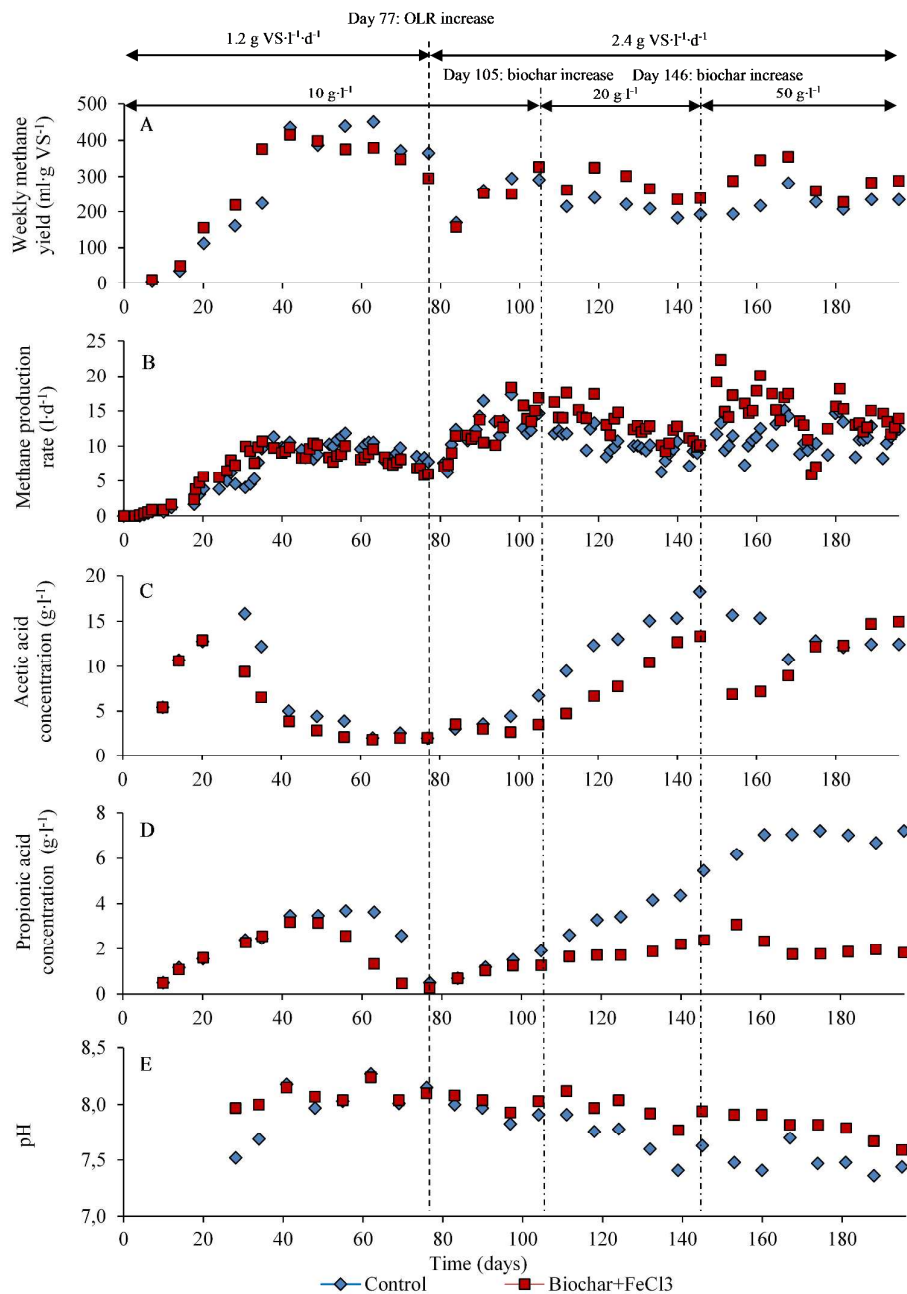
579

580    **Figure 2.** Evolution of the (A) average weekly methane yield, (B) methane production rate,

581    (C) acetic acid concentration, (D) propionic acid concentration and (E) pH in the pilot

582    reactors. The days in which an operational parameter (*i.e.* OLR or biochar concentration) was

583    modified are also indicated (vertical lines)

584

585    **Table 1.** Characteristics of the food waste mixture and the inoculum (9)

| Parameter | Food waste mixture | Inoculum |
|---|---|---|
| TS (%) | 21.0 | 5.81 |
| VS/TS (%) | 90.3 | 59.1 |
| Carbohydrates (g·kg TS$^{-1}$) | 618 | n.m.[1] |
| Proteins (g·kg TS$^{-1}$) | 187 | n.m.[1] |
| Lipids (g·kg TS$^{-1}$) | 121 | n.m.[1] |
| BMPs (ml CH$_4$·g VS$^{-1}$) | 420 | n.m.[1] |
| pH | 5.02 | 8.10 |
| TAN (g·kg TS$^{-1}$) | 0.90 | 5.04 |
| TKN (g·kg TS$^{-1}$) | 30.0 | 93.0 |
| C/N | 16.1 | 3.04 |

586    1. n.m. stands for "not measured"

587

588

589

590

591

592

593

594

595

596

597

598

599

600

601

602

603

604

605

606

607    **Table 2.** Characteristics and composition of the industrial FeCl$_3$ solution

| Parameter | Unit | Value |
|---|---|---|
| **Density at 20 °C** | $(g \cdot cm^{-3})$ | 1.45 |
| **FeCl₃** | (%) | 41.1 |
| **Cl total** | $(g \cdot l^{-1})$ | 397 |
| **Fe total** | $(g \cdot l^{-1})$ | 206 |
| **HCl** | $(g \cdot l^{-1})$ | 2.2 |
| **Mn** | $(mg \cdot l^{-1})$ | 780 |
| **Zn** | $(mg \cdot l^{-1})$ | 390 |
| **Pb** | $(mg \cdot l^{-1})$ | 220 |
| **Ni** | $(mg \cdot l^{-1})$ | 67 |
| **Co** | $(mg \cdot l^{-1})$ | 28 |
| **Cu** | $(mg \cdot l^{-1})$ | 65 |
| **Cr** | $(mg \cdot l^{-1})$ | 45 |
| **Ca** | $(mg \cdot l^{-1})$ | 540 |
| **Na** | $(mg \cdot l^{-1})$ | 110 |
| **Al** | $(mg \cdot l^{-1})$ | 100 |
| **Mg** | $(mg \cdot l^{-1})$ | 15 |

608

609

610

611

612

613

614

615

616

617

618

619

620

621

622

623

624 **Table 3.** Experimental design of the batch experiment. All the reactors were fed with 60 g of

625 FW at an S/X ratio of 1 g VS·g VS$^{-1}$ and incubated at 37 °C

| Reactor | Normalized level | | Real concentrations (g·l$^{-1}$) | |
|---|---|---|---|---|
| | Biochar | FeCl$_3$ | Biochar | FeCl$_3$ |
| 1 | 0 | -1 | 55 | 0.1 |
| 2 | -1 | 1 | 10 | 0.2 |
| 3 | 1 | 1 | 100 | 0.2 |
| 4 | -1 | -1 | 10 | 0.1 |
| 5 | 1 | -1 | 100 | 0.1 |
| 6 | 0 | 1 | 55 | 0.2 |
| 7 | 0 | -1 | 55 | 0.1 |
| 8 | -1 | -1 | 10 | 0.1 |
| 9 | 0 | 1 | 55 | 0.2 |
| 10 | 1 | 1 | 100 | 0.2 |
| 11 | -1 | 1 | 10 | 0.2 |
| 12 | 1 | -1 | 100 | 0.1 |

626

627

628

629

630

631

632

633

634

635

636

637

638

639

640 **Table 4.** Results of the batch experimental design

| Reactor | Methane yield (ml·g VS$^{-1}$) | Maximum methane rate (ml·g VS$^{-1}$·d$^{-1}$) | Time for HPr consumption (d) | Average daily methane production rates (ml·d$^{-1}$)[1] | Final pH |
|---|---|---|---|---|---|
| 1 | 483 | 1327 | 18.9 | 363 | 8.15 |
| 2 | 505 | 948 | 23.0 | 302 | 8.22 |
| 3 | 484 | 1498 | 18.9 | 376 | 8.19 |
| 4 | 509 | 886 | 24.4 | 280 | 8.21 |
| 5 | 489 | 1436 | 18.9 | 374 | 8.18 |
| 6 | 459 | 1249 | 18.9 | 356 | 8.29 |
| 7 | 461 | 1281 | 20.1 | 329 | 8.29 |
| 8 | 501 | 907 | 21.5 | 316 | 8.17 |
| 9 | 456 | 1142 | 20.1 | 323 | 8.29 |
| 10 | 466 | 1489 | 18.9 | 361 | 8.27 |
| 11 | 496 | 913 | 21.5 | 326 | 8.42 |
| 12 | 496 | 1457 | 20.1 | 360 | 8.19 |

641    1. Calculated as final methane yield divided by the time required for HPr consumption (batch duration)

642

643

644

645

646

647

648

649

650

651

652

653

654

655

656

657    **Table 5.** Coefficients of the quadratic model for the main responses of the experimental

658    design

| Parameter/coefficient | Methane yield (ml·g VS$^{-1}$) | Maximum methane rate (ml·g VS$^{-1}$·d$^{-1}$) | Average daily methane production rates (ml·d$^{-1}$)[1] |
|---|---|---|---|
| $a_0$ | 465 | 1250 | 343 |
| $a_{biochar}$ | -9.54[*] | 278.2[**] | 37.3[***] |
| $a_{FeCl3}$ | -9.04[*] | -4.71 | 4.02[***] |
| $a_{biochar-biochar}$ | 28.3[**] | -57.9 | -12.2[***] |
| $a_{biochar-FeCl3}$ | -8.03 | 3.25 | -6.94[***] |
| $R^2$ | 86.7 % | 94.2 % | 100 % |
| p-value Durbin-Wilson | 0.025 | 0.20 | - |

659    1. Calculated as final methane yield divided by the time required for HPr consumption (batch duration)
660    * p-value < 0.05
661    ** p-value < 0.001
662    *** p-value < 0.0001

663

664

665

666

667

668

669

670

671

672

673

674

675

676

677

678
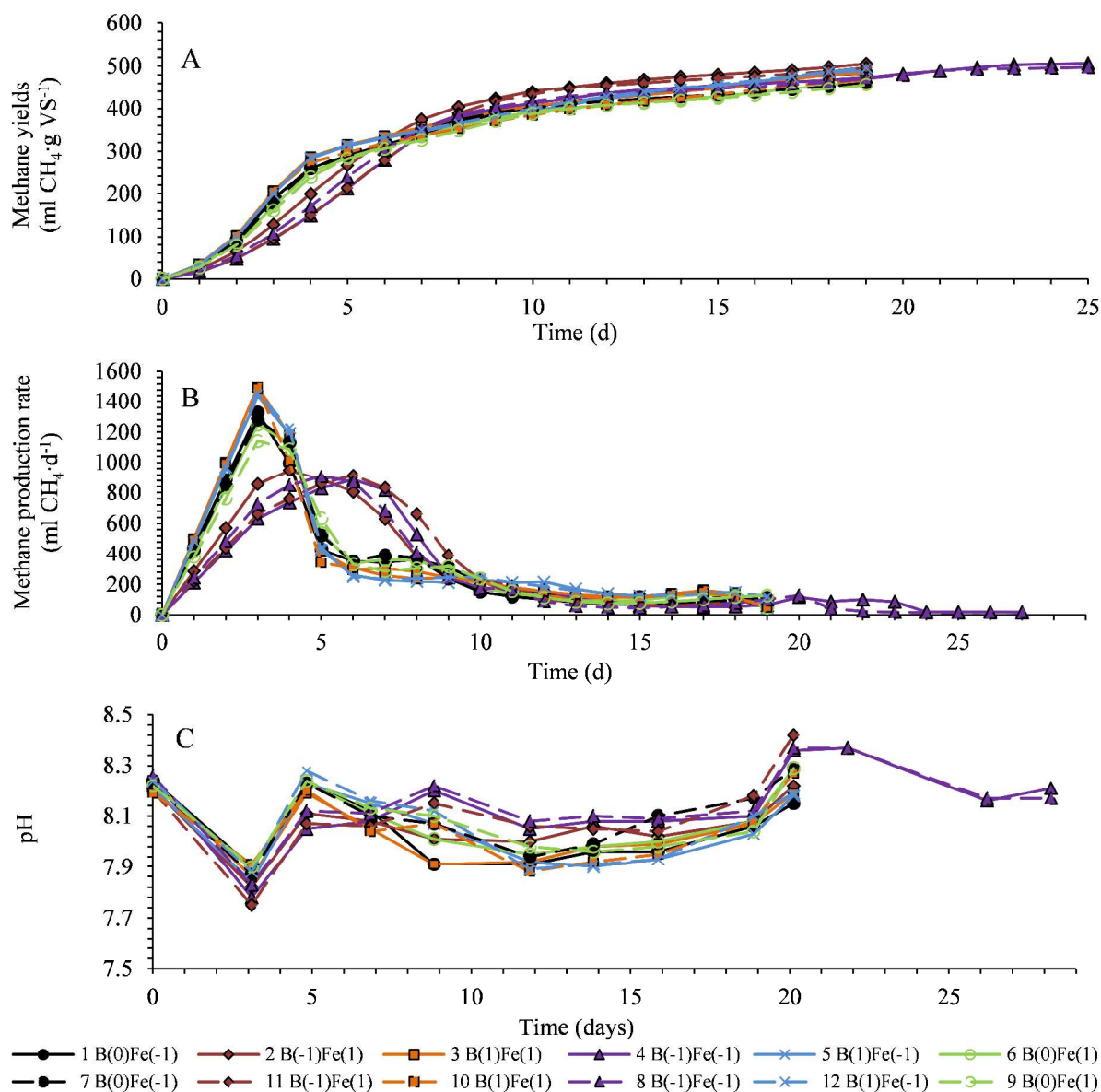
**Figure S1.** Evolution of (A) the methane yields, (B) the methane production rates and (C) the pH

in the reactors. The legend indicates the reactor number and the normalized levels of each factor

(B stands for biochar and Fe for FeCl$_3$ solution)
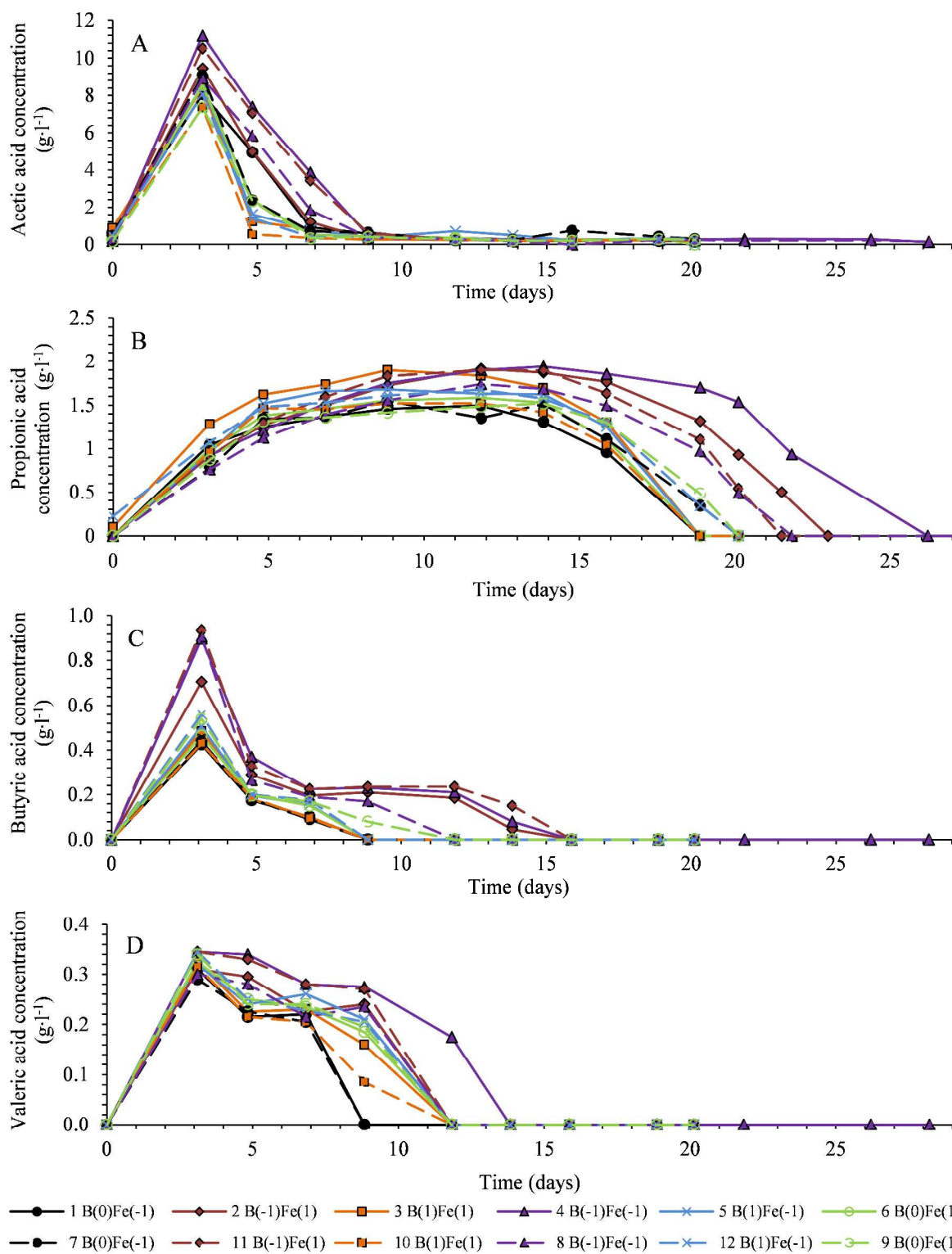
**Figure S2.** Evolution of the concentrations of (A) acetic acid, (B) propionic acid, (C) butyric acid and (D) valeric acid in the reactors. The legend indicates the reactor number and the normalized levels of each factor (B stands for biochar and Fe for FeCl$_3$ solution)